Effects of Soil and Atmospheric Drought on Intra-Annual δ¹³C Patterns in Tree Rings

Valentina Vitali[1,2*], Jernej Jevšenak[3,4], Georg von Arx[2,5#], Marina Fonti[2#], Meisha Holloway-Phillips[2#], Rubén D. Manzanedo[5,6#], Kerstin Treydte[2, 5#], Lorenz Walthert[2#], Roman Zweifel[2#], Matthias Saurer[2]

[1]Forest Ecology, Institute of Terrestrial Ecosystems, Department of Environmental Systems Science, ETH Zürich 8092 Zürich Switzerland

[2]Swiss Federal Institute for Forest, Snow and Landscape Research WSL, 8903 Birmensdorf, Switzerland.

[3]Department of Forest and Landscape Planning and Monitoring, Slovenian Forestry Institute, 1000, Ljubljana, Slovenia

[4]TUM School of Life Sciences, Technical University of Munich, 80333, Freising, Germany

[5]Oeschger Centre for Climate Change Research, University of Bern, Falkenplatz 16, 3012, Bern, Switzerland

[6]Institute of Plant Sciences, University of Bern, 3015, Bern, Switzerland.

1

#Authors listed in alphabetical order.

Email address: valentina.vitali@usys.ethz.ch, valentina.vitali@wsl.ch, Tel.: +41447392840

Abstract

High-resolution carbon isotope ratio ($\delta^{13}C$) measurements of tree rings have the potential to provide seasonal environmental information. However, due to the complexity of the wood formation processes, the reliability of this method for intra-seasonal reconstruction of growing conditions remains unclear. We, therefore, investigated the intra-annual variation of $\delta^{13}C$ in tree rings of three conifer species (*Pinus sylvestris, Picea abies, Abies alba*) across sites from the Swiss Alps to assess their response to seasonal variation of soil water potential (SWP) and vapour pressure deficit (VPD). Intra-annual $\delta^{13}C$ values at a resolution of 10 points per year were assessed using laser-ablation isotope-ratio mass spectrometry. Seasonal $\delta^{13}C$ patterns were analyzed for synchronicity across trees and species, and their correlation with on-site environmental variables was used to determine the driving factors of $\delta^{13}C$, to reconstruct growing season dynamics, and to estimate timings of the growth dynamics and allocation of carbon to xylem formation. The $\delta^{13}C$ patterns showed high synchronicity between species, with characteristic maxima in wet and dry years occurring in the middle of the ring and at the end of the ring, respectively. Seasonal $\delta^{13}C$ variations reliably reflected atmospheric dryness. Higher than normal soil dryness hindered integration of further fresh assimilates into the xylem, thus allowing the identification of species- and site-specific threshold conditions that disrupt wood formation. The $\delta^{13}C$ of Scots pine shows the strongest correlations with VPD and SWP, making it an excellent indicator of environmental variability. Silver fir appears to integrate carbon into xylem structural material over a longer season than the other conifers, whilst Norway spruce shows more plastic site-specific responses to environmental conditions. In conclusion, we identify how atmospheric and soil drought jointly impact tree growth and intra-annual $\delta^{13}C$ patterns across conifer species, offering valuable insights for climate reconstructions and wider applications on forest dynamics.

1. **Introduction**

2

For several decades, stable isotope ratios of tree rings have been successfully used as reliable indicators of environment-plant-interactions (McCarroll & Loader, 2004), for the investigation of spatial hydro-climatic patterns at the continental level (Vitali et al., 2021) and centennial and millennial climate reconstruction (Büntgen et al., 2021; Churakova Sidorova et al., 2020; Treydte et al., 2024). However, most of these studies have an annual or even multi-annual temporal resolution. Due to methodological and interpretation limitations, far less research has been conducted to explore the intra-annual variation in the carbon isotope ratio (δ^{13}C), relating δ^{13}C seasonal dynamics and interactions between phenology and the timing of cell development. These processes play a major role in carbon formation and its integration into wood structures (Castagneri et al., 2017; Cuny et al., 2014a). In conifers, large, thin-walled earlywood tracheids are formed at a high rate in early spring (Cuny et al., 2014a). Smaller, thick-walled latewood cells are built at slower rates but may live up to several months and integrate environmental information over a much longer period (Schollaen et al., 2014). Lignification processes and the use of carbon from storage may further blur cells' environmental information inherited from the carbon used to form them (Kagawa et al., 2006). Earlywood and latewood exhibit distinct anatomical and density characteristics, which significantly influence the intraseasonal δ^{13}C signature in tree rings. These variations can affect the interpretation of carbon isotope records as indicators of physiological processes and environmental conditions. Such anatomical differentiation modulates carbon assimilation and allocation, underscoring the importance of separately analysing EW and LW to improve the accuracy of climate and ecophysiological reconstructions (Belmecheri et al., 2018; Vaganov et al., 2009). However, with a high-resolution analysis, it is possible to study δ^{13}C variations as a continuous variable, thus considering the overlapping integration of carbon across the ring. Nonetheless, understanding the information retained in intra-annual δ^{13}C patterns remains an open challenge, with critical ecological insights waiting to be uncovered.

The variation in δ^{13}C in tree rings provides an integrated record of the ratio of intercellular to atmospheric CO_2 concentrations during the period when the carbon was fixed, reflecting the balance between net CO_2 assimilation and stomatal conductance (Farquhar et al., 1989). Thus, δ^{13}C can be related to canopy functioning and gas exchange, which are directly impacted by environmental factors, with their relative importance depending on the general climate region and site conditions (Gessler et al., 2014). Under optimal conditions, xylem production uses recent assimilates, as sufficient new assimilates are provided by photosynthesis and the phloem transport is fully functional (Gessler et al., 2009). As such, the δ^{13}C of sugars utilized for wood production should integrate seasonal information of growth conditions (Gessler et al., 2014; Helle & Schleser, 2004), with varying latency (Gessler et

3

al., 2009). However, that might not always be the case. Earlywood growth in spring can also be supported by remobilized storage compounds, with this process being more apparent in deciduous trees (Gričar et al., 2022; Helle & Schleser, 2004; Monserud & Marshall, 2001), than in conifers (Martínez-Sancho et al., 2022; Rinne-Garmston et al., 2023). Similarly, radial growth in summer can also depend on remobilized carbon under extreme heat and drought conditions, thus resulting in a decoupling of the $\delta^{13}C$ tree-ring signal from current leaf-level physiology (Hentschel et al., 2016). These results have raised concerns about the impacts of biochemical processes on the intra-annual $\delta^{13}C$ patterns in tree rings. Building on these mechanistic principles, intra-annual $\delta^{13}C$ analyses aim to disentangle finer-scale physiological and environmental signals across the growing season.

Intra-annual $\delta^{13}C$ measurements allow investigating the gradual incorporation of carbon assimilates in woody tissues and the associated environmental signals recorded in tree-ring isotopes (Pérez-de-Lis et al., 2022), and by integrating isotopic measurements with xylogenesis data (Tang et al., 2022), or by comparing intra-annual $\delta^{13}C$ profiles with source water and carbohydrate pools (Michelot-Antalik et al., 2019). Various studies have made use of high-resolution information by measuring tree-ring isotope ratios through laser ablation (Rinne-Garmston et al., 2023; Fonti et al., 2018; Schollaen et al., 2014; Skomarkova et al., 2006) or by manually split tree-rings (Kagawa et al., 2006; Martínez-Sancho et al., 2022), but were often been limited to single sites and species. It remains unknown how consistent these intra-annual isotope signals are between species at a site and between sites, and thus, how reliably the information on environmental conditions can be retrieved. The progress in Laser-Ablation Isotope Ratio Mass-Spectrometry (LA-IRMS), improves the capacity for efficient high-resolution (30μm), detailed and accurate intra-annual data (Saurer et al., 2023), boosting the application potential of intra-annual high-resolution $\delta^{13}C$ analysis.

Tree-ring $\delta^{13}C$ variations are influenced by vapour pressure deficit (VPD), soil moisture (Tang et al., 2022), and drought conditions (Grossiord et al., 2014; Jucker et al., 2017), as plants respond to such conditions by closing their stomata to prevent water loss, especially in low soil water availability conditions, leading to higher $\delta^{13}C$ values in tree rings (Grossiord et al., 2014; O'Leary, 1995). The analysis of $\delta^{13}C$ might, therefore, be a powerful tool for better understanding the combined effects of VPD and soil drought, which are known to affect many forests worldwide in recent decades (Novick et al., 2024). However, extremely dry conditions may not be recorded by $\delta^{13}C$ if they coincide with growth cessation, i.e. stem growth must occur for the $\delta^{13}C$-environmental relationship to be recorded (Barbour & Song, 2014). Conversely, adequate soil water availability reduces $\delta^{13}C$ values by enhancing carbon assimilation (Gavrichkova et al., 2011). Therefore, we can explore seasonal growth

4

kinetics and ^{13}C isotopic composition by accounting for atmospheric and below-ground water availability (Zelenov et al., 2024). A seasonal shape has been shown in another LA-IRMS study, where a **"bell-shaped"** pattern with low δ^{13}C values (Fig.1, blue line) at the edges of the ring and maximum values in the middle was common (Tang et al., 2022). However, dry conditions should significantly modify the δ^{13}C intra-annual pattern (Eglin et al., 2010; Etzold et al., 2022; Helle & Schleser, 2004; Tang et al., 2022; Vaganov et al., 2009), interfering with the integration of the full seasonal trends, thus creating a particular **"monotonic rise"** pattern (Fig.1, red line)**,** where δ^{13}C increases continuously from early to latewood (Xu et al., 2022). We hypothesise that these two δ13C shapes should be identifiable and shared for all species and sites with a clear distinction between wet and dry years (Fig.1). Thus, in generalising this trends the two δ^{13}C shapes should be identifiable and shared for all species and sites with a clear distinction between wetter and drier than normal years (Fig.1). Under moist conditions the δ^{13}C reflected seasonal trends, with lower (more negative) values in spring when conditions are moist and mild (leading to an "open stomata" signal and thus ^{13}C depletion), higher values during summer when it is dry and hot (leading to a "closed stomata" signal, resulting in ^{13}C enrichment), and lower values again in autumn when the environmental conditions return to moist and mild, resulting in a clear **"bell-shaped"** pattern. In the case where δ^{13}C increases continuously from early to latewood, it creates a particular **"monotonic rise"** pattern. Thus, by identifying the different time integrations between the two curves, we can infer the timing of wood formation or early growth stops due to dry conditions.

Species-specific differences should be taken into account as they are associated with inherent genetic differences in water use efficiency and responses to environmental factors (Babst et al., 2013; Brinkmann et al., 2019; Dubbert et al., 2012). Nonetheless, although functional strategies are species-specific, strong synchronicity of the maximum rates of cambial activity between co-existing conifer species has been observed (Cuny et al., 2012), implying that a large part of their wood formation occurs in an overlapping period. Thus, by aligning the start of growing activity with the beginning of stem growth identified by dendrometer measurements can further pinpoint which environmental conditions impact tree growth and ecophysiological mechanisms (Pérez-de-Lis et al., 2022; Zweifel, Sterck, et al., 2021).

To explore the variation of intra-annual δ^{13}C in tree rings and its capacity to record seasonal variability of atmospheric and soil aridity and to tease apart the confounding effect of species-specific responses to environmental conditions, we investigated co-occurring conifer species (Scots pine (*Pinus sylvestris, L.)*, silver fir *(Abies alba, Mill.*), and Norway spruce *(Picea abies, (L.) H. Karst.*), at forest sites varying in water availability.

5

This study benefits from a unique setup in place for the past 10 years, with on-site continuous measurements of environmental variables, including temperature, air moisture and soil water potential, and tree growth monitoring with dendrometers. We pair these variables with high-temporal resolution $\delta^{13}C$ measurements from 10 years of tree rings, totalling 4000 isotope measurements. Following the ecophysiological understanding of $\delta^{13}C$ signals in tree rings, we expect that the dynamic relationship between air and soil moisture and tree physiological functioning is directly linked to the intra-annual variation of $\delta^{13}C$ (Section 3.1). This approach will provide a comprehensive understanding of intra-seasonal dynamics between environmental conditions, tree physiology, and $\delta^{13}C$ variation within tree rings, addressing the following hypothesis:

Hp.1 Common $\delta^{13}C$ intra-annual patterns, shaped by environmental drivers, are consistently observed across different conifer species and sites

Hp.2 The interplay between soil and atmospheric dryness explains the distinct $\delta^{13}C$ variations within annual tree rings.

Hp. 3 The intra-annual environmental changes recorded by $\delta^{13}C$ vary along the ring and provide a temporal link to xylem formation.

2. Methods

2.1. Site and tree species selection

We selected four sites in the Swiss Alps, two in Eastern Grisons (Surava North = Sur_N and Surava South = Sur_S, 1200 m.a.s.l) and two in Central Valais (Buthan= But_N, 800 m.a.s.l., and Lens=Len_S 1000 m.a.s.l.), as pairs of north and south exposed sites (Fig.2a,b, Fig.S.1, Table S.1). The mean annual temperature ranges from ~6°C in the Grisons sites to ~10°C in the Valais sites, and annual precipitation from ~1000 mm in Surava to 600 mm in Valais (1991-2020; MeteoSwiss). In terms of vapour pressure deficit (VPD, kPa) and soil water potential (SWP, kPa), the Valais sites are on average warmer and drier than the Grisons sites, with the Lens site being the driest, and the Sur_N site the wettest and coolest (Fig.2c, S.2). The years 2018, widely regonigsed as a major drought year in Central Europe (Gharun et al., 2020), and 2021 are taken as examples of significantly above average dry and wet year respectively at all sites (Fig.2d, Fig.S.4,5).

We sampled three conifer species, Scots pine (*Pinus sylvestris,* PISY), Norway spruce (P*CAB*), and silver fir (*Abies alba,* ABAL), in the sites with northern exposition (Sur_N, But_N), whereas only Scots pine was present in the sites on south-facing slopes (Sur_S, Len_S). Scots pine, Norway spruce, and silver fir are common

6

coniferous species prevalent in European forests, each playing significant ecological and economic roles. These species exhibit distinct ecophysiological traits and adopt different strategies to withstand environmental stresses, including drought (Bose et al., 2020; Vitali et al., 2017; Walthert & Meier, 2017). Scots pine is adapted to a wide range of soil types and environmental conditions, and it occurs on extreme sites where many other tree species are not able to persist (Bigler et al., 2006). It has low hydraulic conductivity and is known for its isohydric water regulation strategy, maintaining a constant leaf water potential and tight stomatal control during dry conditions (Martínez-Vilalta et al., 2009; Walthert et al., 2024). Norway spruce is known for its vulnerability to dry conditions (Vitali et al., 2017) while it also follows an isohydric strategy, minimizing water loss. However, it has been shown to switch to anisohydric behaviour in extreme droughts (Schumann et al., 2024), thus potentially weakening the drought signal of $\delta^{13}C$ by opening the stomata. Scots pine and Norway spruce have been shown to have similar root systems at Swiss sites (Walthert et al., 2024). On the contrary, silver fir exhibits isohydric behaviour and has a taproot system that provides access to deeper water during dry conditions. Consequently, in general, this species' transpiration remains largely unaffected under drought (Magh et al., 2020), although trees at sites with a higher soil water storage capacity have been shown to have the highest vulnerability to drought (Nourtier et al., 2014), thus potentially weakening the ^{13}C-enrichement connected to drier conditions.

2.2. Environmental data and dendrometer data

Air temperature and relative humidity were measured at hourly time steps using EL-USB-2+ data loggers (Lascar Electronics Ltd., Salisbury, UK). At each of the four study sites, three loggers were mounted on different trees at 2 m height. Values represent the mean of the three loggers. Vapour pressure deficit (VPD) was calculated following Buck, (1981) from temperature and relative humidity. Soil sensors were buried in a soil profile in the central part of each site. In each profile, two to three sensors were embedded at 20 and 80 cm depth (Fig.S.2). Soil water potential (SWP) and soil temperature were recorded at hourly intervals using MPS-2 dielectric sensors and EM-50 data loggers (Decagon Devices, Pullman, WA, USA). This sensor determines SWP indirectly from the measured water content in its porous ceramic sensor, using dielectric permittivity as a proxy for water content. The SWP measurements were temperature-corrected to 22 °C, necessary to remove erroneous temperature effects from the measurements in dry and cold soils following Walthert & Schleppi (2018).

Stem radius changes at breast height were measured with automatic point dendrometers (ZN11-T-WP, Natkon, Oetwil am See, Switzerland) and logged with LORAWAN nodes (Decentlab GmbH, Dübendorf, Switzerland) on

7

two to three trees per site and species. The data were collected in a central Tree-Net database (Zweifel, Etzold, et al., 2021) and processed into the two fractions of growth and tree water deficit (Knüsel et al., 2021; Zweifel et al., 2016). Cored trees (see section 2.3) and trees with dendrometers grew within 20-100 m of the sampled trees.

2.3. Dendrochronological and tree-ring isotope analyses

We took tree cores in October 2022 from five trees per species and site. The removal of resins and other soluble compounds form the cores was achieved through a 24- hour Soxhlet extraction with 96% ethanol using a Soxhlet apparatus (standard 500 ml Soxhlet extractor with dimroth condenser, and 1000 ml round flask, e.g., Carl Roth GmbH + Co, Germany; with an electric heater, ELET36002-18, VWR International (Fonti et al., 2025)). A flat surface was produced with a core microtome (Gärtner & Nievergelt, 2010). Tree-ring widths (TRWs) were measured for ten years from 2013–2022 at 0.01-mm precision on scanned images with the Skippy system (Gärtner et al., 2024), CooRecorder (Maxwell & Larsson, 2021), and cross-dating followed standard procedures (Bunn, 2010; Holmes, 1983). TRW time series (Fig. S.2) showed the largest rings in silver fir in Sur_N (avg. 2.2 mm), followed by But_N (avg. 1 mm), whilst Norway spruce showed similar TRWs at the two sites (avg. 1 mm). Both the rbar and EPS values confirmed high consistency among individual trees for all species and sites. Lower values were obtained for Scots pine at the BUT site, where trees exhibited greater variability in dimensions, however, the trees with highest EPS were selected for the intra-annual measurement (Table S.4). TRWs were used to determine the positions of the sampling shots of a laser mass spectrometer (LA-IRMS). Within each tree ring, we fixed a resolution of 10 (evenly spaced) shots. The $\delta^{13}C$ values of each shot might measure a different number of cells depending on cell size due to the fixed shot width; however, this is considered sufficient to cover the main intra-annual isotope variations (Pérez-de-Lis et al., 2022). The evenly spaced, and tree-ring-width adjusted laser ablation shots ensured that earlywood and latewood were sampled proportionally to their occurrence in each ring, thus minimising anatomical bias across species and years.

The LA-IRMS system consisted of an isotope-ratio mass-spectrometer to measure the stable carbon isotope ratio $\delta^{13}C$ (IRMS, HS2022, Sercon, Crewe, UK), a Cryoflex for the collection of produced CO_2, the ultraviolet-laser with a sample chamber, and controlling software. An elemental analyser for bulk analysis and comparative analyses was also attached to the IRMS (isoEarth, Sercon). The gases and organic dust from whole-wood cores created by the laser ablation were transported with helium through an oven for combustion to CO_2, which was collected with liquid nitrogen traps in the Cryoflex. The collected CO_2 was then released in the IRMS for $\delta^{13}C$

8

measurement. During each sample run, we carried out tests with standard cellulose mats of known isotope ratios to determine the memory and precision of the system ($\pm$0.3 ‰). With 10 years of measurements, two sites with three species, two sites with one species, and five trees per species, we analysed a total of 400 intra-annual $\delta^{13}C$ profiles (ca. 4000 individual $\delta^{13}C$ values). We derived mean annual values of $\delta^{13}C$ in atmospheric CO_2 from NOAA (http://www.esrl.noaa.gov/gmd) and used them to correct the measured $\delta^{13}C$ values. The atmospheric data are available as monthly values, but we considered it too speculative to relate these remote data to our site on such a fine scale. To assess the quality of the developed chronologies, we calculated inter-series correlation coefficients (rbar) and the expressed population signal (EPS; Wigley et al., 1984).

2.4. Data analysis and statistics

2.4.1. Species differences and Day0 alignment

To test for differential sensitivity to environmental variables at each site and each species, we compared the performance in the wettest and dryest years by applying locally estimated scatterplot smoothing (LOESS) to visualize trends in the data and compare patterns across species. LOESS was fitted using a span parameter of 0.75 to balance smoothness and data fidelity (Cleveland et al., 2017). This approach allowed us to capture nonlinear patterns while minimizing overfitting. However, to compare between species and years, we found that a normalization of the beginning of activity was necessary. We used automated dendrometer measurements to identify the start of growth dates each year for each site and each species (Tables S.1), designating this "Day0" as the date of the beginning of the growing season. We accounted for the time lag between the activity start recorded by dendrometers and actual xylem formation. While high-resolution dendrometers allow continuous tracking of stem diameter changes, we recognize that these measurements conflate true radial growth (new cell production) with reversible diurnal and seasonal swelling due to stem hydration, potentially leading to an overestimation of growth onset (Zweifel et al., 2001). However, dendrometers have been validated against microcore sampling and shown to reliably capture growth-onset dates, providing a continuous, non-destructive proxy for cambial phenology (Deslauriers et al., 2007, 2008). This adjustment provided a reliable alignment across different years and species and significantly improved our analyses. Approaches that focus on critical time windows have shown comparative advantages over fixed-length and fixed-time windows (Li et al., 2023). We followed the method proposed by Unterholzner et al., (2024) and constructed a time series aligned by actual growing season that is physiologically relevant and effective in capturing comparably short and variable responses between windows of

9

growth and environmental conditions. We correlated the intra-annual isotope time series with the "Day0"-aligned daily meteorological data. Using this modified time series based on tree functioning periods, rather than fixed calendar periods, we decoupled the environmental variables from calendar dates and translated them into dates preceding or following the start of growth for each year. However, as there are large uncertainties when attempting to identify the end date from dendrometers due to inherent difficulties of assessing an asymptotic curve and due to processes, that post-date xylem formation contributing to swelling and shrinkage later in the year (Deslauriers et al., 2007; Etzold et al., 2022; Zweifel, Etzold, et al., 2021), we left the end date open to be matched with the best cross-correlations with VPD and SWP key physiological constraints on late-season assimilation and growth in conifers, and the most significant variables (Fig.S.12).

2.4.2. Intra-annual variation of the environmental signal recorded by δ¹³C

To investigate the year-to-year variation in intra-annual $\delta^{13}C$ curves and their relationship with environmental conditions, we allocated the 10 sequential sectors of 3-week smoothed time series of environmental variables to the 10 consecutive measurements of $\delta^{13}C$ per year (section 2.4.3), and based on the knowledge of wood formation speed of conifers (Deslauriers et al., 2007; Etzold et al., 2022; Zweifel, Etzold, et al., 2021). These 10 consecutive windows represented the timing and extent of cell formation in each sector of the tree ring. Following (Cuny & Rathgeber, 2016), we assigned a shorter length to the windows allocated to the beginning of the growing season and increasing lengths across the ring, albeit assuming no species-specific differences, and we tested different proportions. We then tested the assumption that different shapes of $\delta^{13}C$ time series correspond to different growing season lengths, as they reflect the recorded environmental conditions (Fig.1). We calculated the cross-correlation between the $\delta^{13}C$ annual curves and seasonal VPD and SWP aggregates by systematically varying the "End date" of the growing season from 15 June to 30 October. We then selected the optimal "End date" of each $\delta^{13}C$-integration (growing) season by identifying the simultaneously highest cross-correlation value between $\delta^{13}C$ and both, VPD and the lowest one between $\delta^{13}C$ and SWP. We then identified the optimal growing-season endpoint as the date that maximized the absolute cross-correlation with VPD while simultaneously minimizing the cross-correlation with SWP. This flexibility implies that the correlation window also varied from year to year, capturing the inter-annual variations in $\delta^{13}C$-integration timing. Once we had identified the optimal $\delta^{13}C$-

10

integration window, we investigated the relationship between $\delta^{13}C$ and the environmental variables at the site level using linear regression models.

2.4.3. Environmental correlations analyses

To investigate the overall relationship of $\delta^{13}C$ with the environmental variables across all years, we calculated running correlations between environmental data and $\delta^{13}C$ values for each shot for all the sampled trees using the *dendroTools* package (Jevšenak & Levanič, 2018) in R (R Core Team, 2022). These were carried out using the shot-level $\delta^{13}C$ data and Day0 aligned daily meteorological data and applying a moving window approach. We tested different lengths of moving windows to evaluate the relationship between the $\delta^{13}C$ data and the environmental variables, as described by Jevšenak & Levanič, (2018), and found the 3-weeks smoothing to be the most suitable weighing for noise to signal variation. We utilized the non-parametric Kendall's tau correlation coefficient, which is particularly suited for handling small sample sizes and data that do not necessarily follow a normal distribution (Gibbons & Chakraborti, 2010). We performed correlations using 3-week aggregated data for all sites and species. When growing season start data were not accessible, average species data were obtained from the TreeNet monitoring network (Etzold et al., 2019). To evaluate the differences in $\delta^{13}C$ values, for each species and between shots throughout the tree ring, we performed variable analyses of variance (ANOVA), Tukey's post hoc tests, and Bonferroni corrections on absolute values of the correlations. Significance was set at $p<0.05$.

3. Results

3.1. Site- and species-specific intra-annual $\delta^{13}C$ patterns

We investigated the intra-annual tree-ring isotopic variation of silver fir, Norway spruce, and Scots pine (respectively ABAL, PCAB, and PISY, Fig.3) in the years 2013 to 2022 by creating high-resolution $\delta^{13}C$ time series through laser-ablation-IRMS based on 10-shots per ring measurements. The intra-annual $\delta^{13}C$ time series showed a strong within-species agreement with mean inter-series correlations of 0.6 on average and EPS values of up to 0.88 (Table S.2). Each species exhibited a clear intra-annual seasonality in the variation of $\delta^{13}C$. The three species showed similar trends in $\delta^{13}C$ values in the first part of the ring but different amplitudes and shapes in the later part of the ring, albeit not strictly attributed to latewood (Fig.S.4). ABAL and PCAB, tended to have lower

11

baseline δ¹³C values than PISY in Sur_N, while in But_N PCAB had the highest δ¹³C values (Fig.3, S.4). For PISY, the latewood at the dry sites (Len_S and Sur_S) was narrower than at the moist sites (Fig.S.4).

When focusing on the very dry (2018), and wet (2021) year, with significantly different VPD and SWP conditions from the mean in June, July, and August at all sites, two distinct intra-seasonal patterns emerged (Fig.4): the **"bell shape"** with low δ¹³C values in the earlywood (shots ~1-4), followed by increasing values in the middle stages of the ring, followed by a decline in the latewood (shots ~7-10) is associated with moist years; the **"monotonic raise"** pattern with similarly low δ¹³C values in the earlywood followed by a steep increase and maximum values in the latewood, i.e. lacking the late downward trend can be seen in the dry years. The two shapes were common between species at all sites, with two exceptions: at the moist Sur_N site PISY and ABAL preserved the bell shape even in the dry years, and the driest site Len_S, only showed a partial bell shape in wet years (Fig. 4).

3.2. Optimal temporal window

To identify the strongest integration of environmental signal in the δ¹³C variation, we identified the temporal window length with the highest cross-correlation results between the intra-annual δ¹³C and the Day0-anchored environmental variables. In general, δ¹³C followed the VPD trend closely and had a clear inverse relationship to SWP (Fig.5). The maximum correlations occurred mostly in the summer months or later in autumn but showed a strong year-to-year variation (Fig.S6). Focusing on the dry year 2018, which showed the lowest SWP and highest VPD conditions at all sites, and the wet year 2021, we observed species-specific differences in the identified optimal temporal windows, although the two shapes connected to the dry and wet years remain common across species. We observed negative δ¹³C–SWP correlations, a match with VPD and minimal season-length variation in the drought year of 2018 for all other species and sites (Fig.S6, S.7), with the exception of ABAL, which consistently showed the latest End dates and δ¹³C bell shapes, indicating that xylem formation extended into the cooler, moister autumn conditions (Fig.5, S.6,S.7). PCAB showed strong year-to-year variation from mid-July to September, with a negative relationship to VPD (Fig.5, S.6,S.7). PISY in Len_S and Sur_S show sharp monotonic rise pattern linked to a July End date. On the contrary, in the moist year of 2021, most species displayed a bell-shaped δ¹³C curve, with End dates around mid-August. Interestingly, PISY at Sur_S had an earlier End date in 2021, likely due to plummeting SWP in the early season, unlike at other sites where VPD levelled off mid-season. On the contrary, PISY in Len_S showed a strong delay in the maximum cross-correlation in 2021, with a plateau in δ¹³C first emerging in the middle of the ring, followed by a new increase, following closely VPD and SWP

12

patterns, indicating a moist period halfway through the season, followed by a new dry period, thus leading to a new increase in $\delta^{13}C$ values.

3.3. Correlation of intra-annual tree-ring $\delta^{13}C$ with SWP and VPD

We observed a strong, year-to-year relationship between $\delta^{13}C$ and the environmental variables, allowing us to quantify the intra-annual consistency of these relations across sites and species. The correlations between tree-ring $\delta^{13}C$ and both VPD and SWP improved significantly after the alignment to Day0 and End dates, indicating a more accurate reflection of the incorporated environmental signal in the tree-ring carbon (Fig.6,S.8). Without these alignments, the calendar-dates bound relationships of $\delta^{13}C$ with the environmental variables were weaker, although the positive correlation of $\delta^{13}C$ with VPD was partially captured (Fig.S.8). Across all sites and species, there was a positive correlation between VPD and $\delta^{13}C$, with the R² values ranging from 0.29 to 0.46 (Fig.6). The sites Len_S and Sur_N display the steepest slopes (0.145 and 0.142, respectively), suggesting a strong control of VPD on $\delta^{13}C$ at these locations. Conversely, a negative correlation was observed between SWP and $\delta^{13}C$. As SWP became more negative (indicating drier soil conditions), $\delta^{13}C$ values tended to become less negative. The R² values were generally higher for the south-exposed sites and ranged widely, from 0.07 for ABAL in BUT_N to 0.72 for PISY in Len_S. The strong correlation of PISY at Len_S points to the substantial influence of SWP on $\delta^{13}C$ at this site. The moist site of Sur_N showed the steepest negative slope, where a small change to lower SWP led to a relatively large increase in $\delta^{13}C$, albeit at higher absolute values than at the drier site. These findings underscore the influence of local site conditions and species-specific characteristics on $\delta^{13}C$ values in response to VPD and SWP, but also the strong general trends that become apparent once the timing of xylem formation has been identified.

3.4. Day0 aligned correlation analysis and shot-level climate signal

The strength of high-resolution measurement of $\delta^{13}C$ is the access to cell-level measurements along the ring. Thus, the traditional correlation of tree-ring variations with environmental variables can be performed for each shot. We evaluate the recorded signal in the $\delta^{13}C$ intra-annual variation for the measured 10 years, through a moving window correlations approach, by aligning each year to the beginning of growth activity (Day0 alignment is indicated by the solid line in Fig.7, all sites in S.10). We calculated the $\delta^{13}C$ correlations with environmental data

13

for each measured shot for the on-site measured variables (temperature, air humidity, soil moisture and soil temperature, Fig.S.11), and tested the common approach of using calendar-based datasets (Fig.S.12), however, the correlations with Day0 alignment were significantly stronger. Consistently positive correlation patterns during the mid to late growing season appear between $\delta^{13}C$ and VPD for most species, with an overall median correlation of 0.6, and consistently negative correlation patterns emerged between $\delta^{13}C$ and SWP, with an overall median correlation of -0.4. On average, shots showed similar correlations in groups of three for both variables. The major differences in the shot-level correlations can be seen in shots 8-10, which included mostly latewood material (Fig.S.13, S.14, Table S.4). PISY, occurring at all four sites, thus covering the largest environmental gradient, represents the main visible trend along the shots: one with a sign change in the correlations in the last two shots of the ring (Fig.7 a,b, But_N), the other with a gradual temporal shift of highest correlations from early to late shots (Fig7 e,f,g,h, in the dry sites of Sur_S and Len_S), or, finally, a general lack of strong correlations trends (Fig.7c, Sur_N).

4. Discussion

4.1. Common intra-annual tree-ring $\delta^{13}C$ patterns between conifer species, dependent on wet and dry seasonal patterns

In this study, we investigated the intra-annual $\delta^{13}C$ patterns in tree rings for silver fir, Norway spruce, and Scots pine in two pairs of sites in two Swiss regions over a 10-year period to assess the environmental and physiological signals stored in wood isotopic ratios. Using a multi-species approach at locations varying in water availability enabled us to tease apart the dominant environmental factors and identify the confounding effect of species and site of $\delta^{13}C$-environmental patterns. Although distinct species-specific differences could be shown in the average rates of $\delta^{13}C$ (Fig.3, Fig.S.4), common intra-annual patterns across species and sites were linked to atmospheric and soil dryness. We observed a strong agreement in intra-annual $\delta^{13}C$ within sites and between species, especially in the wettest conditions (Table S.2,3), in agreement with **Hp1.** This consistency is an important prerequisite for the widespread application of high-resolution isotope analyses to better understand the effects of drought on forest trees.

The wet year and north-facing sites showed most consistently a bell-shaped $\delta^{13}C$ pattern, as water limitation is rare (Fig.4), species differences in stomatal regulation are minimized (Schumann et al., 2024), and cambial activity is more synchronised (Cuny et al., 2012). This is consistent with findings of other high-resolution intra-annual

14

investigations of Scots pine in Scandinavia e.g. (Rinne-Garmston et al., 2023; Soudant et al., 2016; Tang et al., 2022), for Norway spruce in another intra-annual study at a cool and moist alpine site (Martínez-Sancho et al., 2022). All three species in the moist site of Sur_N show the highest growth rates (Fig. S.2) and a common bell shape (Figs.3,5), suggesting a strong overlap of the canopy functioning of the three species, a clear shared environmental signal recorded, and no strong water limitation effects. Where differences in the intra-annual δ^{13}C pattern did occur, this may be attributable to differences in the time span of stem growth activity (Etzold et al., 2019). Scots pine and spruce show a good season-integration match in mid-August, while silver fir showed a stronger decline in δ^{13}C in the later part of the ring (Fig.5), suggesting that the carbon used in the latewood is formed under cool and moist conditions, likely reflecting xylem production and lignification extending later in the autumn period. The 2 ‰ higher average δ^{13}C in the later shots in pine and spruce further suggests the use of carbon formed in warmer and drier conditions for the formation of that woody tissue, and thus an earlier cessation of xylem formation compared with silver fir (Fig.3,4).

The wet years showed the common bell shape, while in dry years, the intra-annual pattern changed drastically from a bell shape to a monotonic rise pattern, i.e., the maximum isotope values were found in the latest cells (Fig. 4, 5). Under drought, trees minimize water loss via stomatal closure, resulting in ^{13}C-enriched assimilates (Gessler et al., 2009; McCarroll & Loader, 2004). Simultaneously, cambial downregulation slows cell division and wall formation, reducing the sink strength for new assimilates (Hommel et al., 2016). Additionally, phloem flow is restricted, limiting the transport of enriched sugars to the cambium (Winkler & Oberhuber, 2017). This leads to diminished incorporation of fresh photosynthates in latewood, or even a complete shift to stored reserves or a complete arrest of growth (Rathgeber, 2017). Thus, when VPD is highest and SWP is critically low like in 2018, the trees experience rapid and more severe stomatal responses and stomatal closure earlier in the growing season (Grossiord et al., 2020; Petek-Petrik et al., 2023), truncating the carbon assimilation period (Pflug et al., 2015), which together with turgor limitation, results in the cessation of production of new cells (Cabon et al., 2020; Mitchell et al., 2014; Peters et al., 2021; Zweifel, Sterck, et al., 2021), resulting in the observed monotonic rise pattern (Fig.4). The year 2018, is a well-known drought year in the study region that negatively affected forest productivity by 20% in Switzerland (Gharun et al., 2020), thus supporting our assumption of an early stop of xylem production. However, silver fir is the only species not showing a monotonic rise pattern in 2018 at the Sur_N site, indicating only a minor impact of this drought year on this species. This observed dependency of inter-annual variation in δ^{13}C on wet and dry conditions aligns with our conceptual diagram and **Hp2**, showing the

15

direct interplay between soil and atmospheric dryness converging to create distinct $\delta^{13}C$ patterns within annual tree rings in conifer trees.

In our case, the strong agreement of $\delta^{13}C$ curves between trees of the same species supports the environmental-driven $\delta^{13}C$ signal in conifers. As earlywood production in conifers is influenced by stored compounds only to a minor degree (Barbour et al., 2002; Dickmann & Kozlowski, 1970), the $\delta^{13}C$ variations may better reflect current growing season conditions than in deciduous species (Monson, Littlejohn, et al., 2018; Monson, Szejner, et al., 2018). This common pattern appears to be distinctly different from the one of broadleaf deciduous trees, which have been shown to have a seasonally recurring tri-phase carbon isotope pattern, with (i) the highest values of $\delta^{13}C$ in the earlywood (of up to 5‰ higher), followed by (ii) a decline and plateau, with minimum $\delta^{13}C$ values occurring in the latewood and (iii) a gradual increase of $\delta^{13}C$ values at the very end of each tree ring, linked to changes in downstream processes of carbohydrate metabolism, and strongly connected to the shifts in heterotrophic and autotrophic mechanisms that support wood formation (Helle & Schleser, 2004; Offermann et al., 2011).

4.2. Finding the activity window and limiting factors: VPD drives the intra-annual $\delta^{13}C$ variation, and SWP triggers growth cessation

One of the challenges in the interpretation of intra-annual $\delta^{13}C$ values is relating them to the timing of growth, which varies from year to year. However, here we show that isotope patterns can, in fact, help us to infer growth dynamics through the recording of environmental stressors on tree physiology. The relationship between $\delta^{13}C$ and VPD and SWP, after alignment to the Day0 and End dates (Fig.6), shows significantly improved correlations with $\delta^{13}C$ values for both VPD and SWP, thus providing the opportunity to connect environmental variables with $\delta^{13}C$ variations. Other research has shown that deriving an optimal period of correlation between $\delta^{13}C$ values and local environmental data leads to a more accurate prediction of intra-annual variation in tree responses (Castagneri et al., 2017; Soudant et al., 2016; Zhang et al., 2012; Ziaco, 2020). Soudant et al. (2016) showed that an optimized time-frame approach based on the timing of key phenological stages, such as cell formation, improved the linear regressions between $\delta^{13}C$ and local environmental variables (i.e., light availability in Scandinavia). Thus, by accounting for statistically optimized periods, we not only improve the predictive power of $\delta^{13}C$ variation on both intra- and inter-annual scales but also provide a direct time-space link in the wood structure and quantify the effective contribution of the environmental variables to the $\delta^{13}C$ variation paving the way to a more mechanistic understanding of tree-ring carbon deposition.

16

A consistent positive relationship of VPD with δ^{13}C was shown regardless of species and position within the tree ring, thus supporting the link between canopy functioning and seasonal variation in δ^{13}C in the xylem (Fig.6). This is in accordance with the findings by Zweifel et al., (2021) based on dendrometer-measured stem growth data at the same sites. The SWP relationship with δ^{13}C was more site-dependent (Fig.6). The differences in intercepts and ranges do indicate species-specific adaptations like isohydricity or different niche rooting systems, however, the overall pattern remains consistent. The moist site of Sur_N showed the steepest negative slope, indicating that a small change of lower SWP leads to a relatively large increase in δ^{13}C. This suggests that it is not the absolute drop in SWP that can lead to the interruption of xylem formation but rather the site-relative drop. This was apparent in the 2018 drought when a monotonic rise pattern occurred in all sites, including the wettest site of Sur_N (but for ABAL at Sur_N, Fig.8). There we observed significantly lower VPD and higher SWP than at all the other sites; while all sites commonly reached values of -1000kPa, the minimum SWP in Sur_N reached in 2018 was -150 kPa at 80 cm depth, and -700 kPa at 20cm depth (Fig.1, S.1). In the other years, SWP at Sur_N generally only reached a minimum of -40 kPa at 80 cm and -300 kPa at 20cm depth, suggesting uncharacteristically dry conditions of the 2018 growing season leading to an early end of xylem production. Meanwhile, we observed bell-shaped curves in other years (e.g. 2019, 2022), even though VPD was higher than in 2018, but SWP was not lower. Notably, Sur_N is a relatively cold site thus, the rooting depth and root density could be reduced due to characteristic low soil temperatures. Therefore, already a slight drop in soil water potential could have a relatively high negative impact on growth because of a relatively strong reduction of water uptake.

Overall, our results suggest that although VPD drives the seasonal variation in δ^{13}C in tree rings, by influencing stomatal closure and photosynthetic rates, the cessation of growth is connected to the synchronization of atmospheric and below-ground dryness (Etzold et al., 2022), with soil water availability as the factor that can induce an abrupt stop in xylem production. If SWP is not significantly lower than in other years, trees are acclimated to the site conditions and can carry on with growth until autumn, even at high VPD (Etzold et al., 2019), provided that enough soil water is available for stem growth. Thus, we conclude that by identifying the timing of the growth period, we can identify not only the environmental drivers of δ^{13}C variation (**Hp3**) but also the potential trigger of early growth cessation at both dry and moist sites. This cross-site consistency suggests a generalizable pattern in conifer drought physiology, where VPD primarily modulates isotopic discrimination and SWP governs growth cessation timing, modulated by rooting depth and soil moisture buffering capacity.

4.3. Within-ring δ^{13}C variation reflects temporal shifts in environmental signal integration

17

Environmental information stored in tree rings changes from early to latewood reflect, on the one hand, the seasonal changes in the factors driving cell production (Castagneri et al., 2017) and, on the other hand, the lag in the integration of canopy assimilates into the xylem tissue, which depends on the stage of growth during the growing season (Cuny et al., 2014b; Gessler et al., 2009; Rossi et al., 2014). High-resolution measurements of $\delta^{13}C$ allowed us to identify of intra-annual changes in seasonal signal integration along tree rings, with significant differences between the first and last part of the ring, and significant changes at the 4th and 8th shots (Fig.S.13, S.14). These points of transition represent critical periods in wood formation, when the trees are particularly sensitive to environmental changes, supporting our hypothesis that the strength of the correlation between $\delta^{13}C$ environmental variables differs across the ring (**Hp3**). The strength of the $\delta^{13}C$ correlations with environmental conditions is dependent upon both the physiological responses of photosynthetic and post-photosynthetic carbon isotope discrimination, but also on the amount of living tissue at each time point (Soudant et al., 2016; Wieloch et al., 2024). It has been shown that a large number of wood cells are usually formed simultaneously in early summer, which is consistent with the findings that the critical period for maximum rates of cell division occurs around the summer solstice in temperate and boreal forests (Balducci et al., 2016; Carrer et al., 2017; Gričar et al., 2022). These periods of rapid cell division result in a heightened sensitivity to summer atmospheric conditions, as also shown in whole-ring width series (Belokopytova et al., 2019; Carrer et al., 2017, 2018; Zelenov et al., 2024). In annually resolved isotope records, this could lead to the amplification of early summer signals and the attenuation of late-season signals, especially under stressful conditions where cambial activity may go undetected (Pérez-de-Lis et al., 2022; Pflug et al., 2015). The distinction between early and late wood is a good first estimation of the intra-annual variation of carbon assimilation (Fig. S3.b). For example, Norway spruce showed the highest annual $\delta^{13}C$ values in But_N, while Scots Pine was the one with the highest values in Sur_N, identifying potential acclimation differences between the sites. However, through high-resolution interannual analyses, such as in this study, we can identify the multiple shifts in the strength and direction of the environmental signals throughout the growth year. For example, Silver fir exhibited a pronounced bell-shaped intra-annual $\delta^{13}C$ pattern even under drought conditions, whereas Scots pine and Norway spruce shifted to a monotonic rise pattern in $\delta^{13}C$ values. This difference can be partly attributed to the silver fir's deeper and more extensive root system, which allows sustained access to subsoil moisture through mid-season (Brunner et al., 2015). By contrast, Norway spruce, which concentrates roots in shallower soil horizons, experiences more rapid declines in water uptake as surface layers dry (Puhe, 2003). Moreover, Silver fir displays a relatively anisohydric stomatal strategy, delaying closure despite rising vapour-pressure deficit, which prolongs discrimination against ^{13}C into the late summer (Peters et al., 2019).

18

Scots pine at the But_N site showed a switch from negative to positive correlations between $\delta^{13}C$ values and environmental variables in the 8-10th shots for all species (Fig.7 a,e). These shots captured latewood material, and the substantial differences in $\delta^{13}C$ values may be due to the transition from growth-limiting to growth-promoting effects of warmer temperatures during the later stages of the growing season. On the contrary, at the dry sites Scots pine showed a distinct temporal link of the $\delta^{13}C$ correlation with VPD and SWP, where the shot-level strongest correlations followed the advancement of the growing season, producing a clear "diagonal" of maximum correlations (Fig.7e,f,g,h). This underscores its sensitivity to VPD and SWP but also its reliance on fresh assimilates that can record seasonal variations (Barbour et al., 2002; Kress et al., 2009). As such, Scots pine is a highly promising species to record intra-annual variation in VPD and SWP.

In this study, we introduce a novel, integrated approach that combines high-resolution carbon isotope analysis with daily climate correlation (Jevšenak, 2019). This framework enables us to resolve intra-annual isotope variations and to pinpoint the timing of seasonal climatic influences. We recognize, however, that our ten-year dataset, while substantial in raw data volume, represents a relatively short series for correlation analysis, which can lead to inflated coefficients (Torbenson et al., 2024). To mitigate this, we employed the more conservative Kendall's tau metric. Moreover, the detected climate–carbon relationships align with the expected seasonal windows, lending confidence to our results. Finally, because of the limited time span, we did not assess potential carry-over effects, which could further clarify the dynamics of climate–carbon interactions (Andreu-Hayles, 2022).

5. Conclusions

By understanding the relationship between environmental variability and $\delta^{13}C$ variation at a high resolution, we enhanced the interpretation of information stored within tree rings and highlighted the direct temporal link between wood formation and growing conditions. While we find a very strong and consistent VPD signal across all sites and species, we also show that SWP plays a key role in the interruption of growth processes, regardless of the minimum values reached (i.e. a small relative drop in SWP at a moist site has a more dramatic impact on the $\delta^{13}C$ signal than recurring dry conditions at a drier site). These findings help in understanding the effects of soil drought and VPD on trees under increasing climate change impacts. This understanding may

19

furthermore be useful to inform ecosystem-level carbon sequestration models based on future climate scenarios of potential thresholds in soil or air dryness that impeach growth and thus limit carbon sequestration, meanwhile, the consistent VPD signal across species and sites offers a high potential for reconstructions of summer conditions. Scots pine, in particular, shows high potential, owing to its large distribution and strong connection to current-year assimilates, although further research is needed to investigate the consistency of this signal across its full range of occurrence. Finally, high-resolution intra-annual changes in $\delta^{13}C$ can be particularly useful on sites and in times with no access to instrumental data as $\delta^{13}C$ patterns show strong commonality across sites and reflect the combined impact of atmospheric and soil dryness. Further comparisons between various temporal and spatial scales, but also across species and stand dynamics, are now needed to deepen our understanding of how trees respond to climate change and how they incorporate physiological responses to environmental conditions in their tree rings.

Authors contributions

V.V. and M.S. conceived and designed the study. V.V. and J.J. analysed the data and wrote the manuscript. G.v.A., M.F., M.H.-P., R.D.M., K.T., L.W., and R.Z. contributed equally to the manuscript revision. All authors reviewed and approved the final manuscript.

Data availability

 The data and code that support the findings of this study are openly available in ENVIDAT at https://www.doi.org/10.16904/envidat.564.

20

UNCORRECTED MANUSCRIPT

Conflict of Interest

None declared

Data Availability Statement

The data and code that support the findings of this study are openly available in ENVIDAT at
https://www.doi.org/10.16904/envidat.564.

21

References

Andreu-Hayles, L. (2022). Limits and Strengths of Tree-Ring Stable Isotopes. In M. Lévesque, R. Guerrieri, R. T. W. Siegwolf, & C. Körner, *Tree Physiology* (pp. 399–428). Springer International Publishing. https://doi.org/10.1007/978-3-030-92698-4_14

Babst, F., Poulter, B., Trouet, V., Tan, K., Neuwirth, B., Wilson, R., Carrer, M., Grabner, M., Tegel, W., Levanic, T., Panayotov, M., Urbinati, C., Bouriaud, O., Ciais, P., & Frank, D. (2013). Site- and species-specific responses of forest growth to climate across the European continent. *Global Ecology and Biogeography*, *22*(6), 706–717. https://doi.org/10.1111/geb.12023

Balducci, L., Cuny, H. E., Rathgeber, C. B. K., Deslauriers, A., Giovannelli, A., & Rossi, S. (2016). Compensatory mechanisms mitigate the effect of warming and drought on wood formation. *Plant, Cell & Environment*, *39*(6), 1338–1352. https://doi.org/10.1111/pce.12689

Barbour, M. M., & Song, X. (2014). Do tree-ring stable isotope compositions faithfully record tree carbon/water dynamics? *Tree Physiology*, *34*(8), 792–795. https://doi.org/10.1093/treephys/tpu064

Barbour, M. M., Walcroft, A. S., & Farquhar, G. D. (2002). Seasonal variation in δ13C and δ18O of cellulose from growth rings of Pinus radiata. *Plant, Cell and Environment*, *25*(11), 1483–1499. https://doi.org/10.1046/j.0016-8025.2002.00931.x

Belmecheri, S., Wright, W. E., Szejner, P., Morino, K. A., & Monson, R. K. (2018). Carbon and oxygen isotope fractionations in tree rings reveal interactions between cambial phenology and seasonal climate. *Plant, Cell and Environment*, *41*(12), 2758–2772. https://doi.org/10.1111/pce.13401

Belokopytova, L. V., Babushkina, E. A., Zhirnova, D. F., Panyushkina, I. P., & Vaganov, E. A. (2019). Pine and larch tracheids capture seasonal variations of climatic signal at moisture-limited sites. *Trees*, *33*(1), 227–242. https://doi.org/10.1007/s00468-018-1772-2

Bigler, C., Bräker, O. U., Bugmann, H., Dobbertin, M., & Rigling, A. (2006). Drought as an Inciting Mortality Factor in Scots Pine Stands of the Valais, Switzerland. *Ecosystems*, *9*(3), 330–343. https://doi.org/10.1007/s10021-005-0126-2

22

Bose, A. K., Gessler, A., Bolte, A., Bottero, A., Buras, A., Cailleret, M., Camarero, J. J., Haeni, M., Hereş, A.-M., Hevia, A., Lévesque, M., Linares, J. C., Martinez-Vilalta, J., Matías, L., Menzel, A., Sánchez-Salguero, R., Saurer, M., Vennetier, M., Ziche, D., & Rigling, A. (2020). Growth and resilience responses of Scots pine to extreme droughts across Europe depend on predrought growth conditions. *Global Change Biology*, *26*(8), 4521–4537. https://doi.org/10.1111/gcb.15153

Brinkmann, N., Eugster, W., Buchmann, N., & Kahmen, A. (2019). Species-specific differences in water uptake depth of mature temperate trees vary with water availability in the soil. *Plant Biology (Stuttgart, Germany)*, *21*(1), 71–81. https://doi.org/10.1111/plb.12907

Brunner, I., Herzog, C., Dawes, M. A., Arend, M., & Sperisen, C. (2015). How tree roots respond to drought. *Frontiers in Plant Science*, *6*, 547. https://doi.org/10.3389/fpls.2015.00547

Buck, A. L. (1981). New Equations for Computing Vapor Pressure and Enhancement Factor. *Journal of Applied Meteorology*, *20*(12), 1527–1532. https://doi.org/10.1175/1520-0450(1981)020<1527:NEFCVP>2.0.CO;2

Bunn, A. G. (2010). Statistical and visual crossdating in R using the dplR library. *Dendrochronologia*, *28*(4), 251–258. https://doi.org/10.1016/j.dendro.2009.12.001

Büntgen, U., Urban, O., Krusic, P. J., Rybnicek, M., Kolar, T., Kyncl, T., Ac, A., Konasova, E., Caslavsky, J., Esper, J., Wagner, S., Saurer, M., Tegel, W., Dobrovolny, P., Cherubini, P., Reinig, F., & Trnka, M. (2021). Recent European drought extremes beyond Common Era background variability. *Nature Geoscience*, *14*, 190-+.

Cabon, A., Peters, R. L., Fonti, P., Martínez-Vilalta, J., & de Cáceres, M. (2020). Temperature and water potential co-limit stem cambial activity along a steep elevational gradient. *New Phytologist*, *226*(5), 1325–1340. https://doi.org/10.1111/nph.16456

Carrer, M., Castagneri, D., Prendin, A. L., Petit, G., & Von Arx, G. (2017). Retrospective Analysis of Wood Anatomical Traits Reveals a Recent Extension in Tree Cambial Activity in Two High-Elevation Conifers. *Frontiers in Plant Science*, *8*, 737. https://doi.org/10.3389/fpls.2017.00737

23

Carrer, M., Unterholzner, L., & Castagneri, D. (2018). Wood anatomical traits highlight complex temperature influence on Pinus cembra at high elevation in the Eastern Alps. *International Journal of Biometeorology*, *62*(9), 1745–1753. https://doi.org/10.1007/s00484-018-1577-4

Castagneri, D., Fonti, P., Von Arx, G., & Carrer, M. (2017). How does climate influence xylem morphogenesis over the growing season? Insights from long-term intra-ring anatomy in *Picea abies*. *Annals of Botany*, mcw274. https://doi.org/10.1093/aob/mcw274

Churakova Sidorova, O. V., Corona, C., Fonti, M. V., Guillet, S., Saurer, M., Siegwolf, R. T. W., Stoffel, M., & Vaganov, E. A. (2020). Recent atmospheric drying in Siberia is not unprecedented over the last 1,500 years. *Scientific Reports*, *10*(1), 15024. https://doi.org/10.1038/s41598-020-71656-w

Cleveland, W. S., Grosse, E., & Shyu, W. M. (2017). Local regression models. In *Statistical models in S* (pp. 309–376). Routledge.

Cuny, H. E., & Rathgeber, C. B. K. (2016). Xylogenesis: Coniferous Trees of Temperate Forests Are Listening to the Climate Tale during the Growing Season But Only Remember the Last Words! *Plant Physiology*, *171*(1), 306–317. https://doi.org/10.1104/pp.16.00037

Cuny, H. E., Rathgeber, C. B. K., Frank, D., Fonti, P., & Fournier, M. (2014a). Kinetics of tracheid development explain conifer tree-ring structure. *New Phytologist*, *203*(4), 1231–1241. https://doi.org/10.1111/nph.12871

Cuny, H. E., Rathgeber, C. B. K., Frank, D., Fonti, P., & Fournier, M. (2014b). Xylogenesis and Phenological Timings in Coniferous Trees. *New Phytologist*, *202*(4), 1235–1245. https://doi.org/10.1111/nph.12716

Cuny, H. E., Rathgeber, C. B. K., Lebourgeois, F., Fortin, M., & Fournier, M. (2012). Life strategies in intra-annual dynamics of wood formation: Example of three conifer species in a temperate forest in north-east France. *Tree Physiology*, *32*(5), 612–625. https://doi.org/10.1093/treephys/tps039

Deslauriers, A., Rossi, S., & Anfodillo, T. (2007). Dendrometer and intra-annual tree growth: What kind of information can be inferred? *Dendrochronologia*, *25*(2), 113–124. https://doi.org/10.1016/j.dendro.2007.05.003

24

Deslauriers, A., Rossi, S., Anfodillo, T., & Saracino, A. (2008). Cambial phenology, wood formation and temperature thresholds in two contrasting years at high altitude in southern Italy. *Tree Physiology*, *28*(6), 863–871. https://doi.org/10.1093/treephys/28.6.863

Dickmann, D. I., & Kozlowski, T. T. (1970). Mobilization and incorporation of photoassimilated $\delta^{14}C$ by growing vegetative and reproductive tissues of adult Pinus resinosa Ait. Trees. *Plant Physiology*, *45*, 284–288.

Dubbert, M., Rascher, K. G., & Werner, C. (2012). Species-specific differences in temporal and spatial variation in δ13C of plant carbon pools and dark-respired CO2 under changing environmental conditions. *Photosynthesis Research*, *113*(1–3), 297–309. https://doi.org/10.1007/s11120-012-9748-3

Eglin, T., Francois, C., Michelot, A., Delpierre, N., & Damesin, C. (2010). Linking intra-seasonal variations in climate and tree-ring δ13C: A functional modelling approach. *Ecological Modelling*, *221*(15), 1779–1797. https://doi.org/10.1016/j.ecolmodel.2010.04.007

Etzold, S., Sterck, F., Bose, A. K., Braun, S., Buchmann, N., Eugster, W., Gessler, A., Kahmen, A., Peters, R. L., Vitasse, Y., Walthert, L., Ziemińska, K., & Zweifel, R. (2022). Number of growth days and not length of the growth period determines radial stem growth of temperate trees. *Ecology Letters*, *25*(2), 427–439. https://doi.org/10.1111/ele.13933

Etzold, S., Ziemińska, K., Rohner, B., Bottero, A., Bose, A. K., Ruehr, N. K., Zingg, A., & Rigling, A. (2019). One Century of Forest Monitoring Data in Switzerland Reveals Species- and Site-Specific Trends of Climate-Induced Tree Mortality. *Frontiers in Plant Science*, *10*, 307. https://doi.org/10.3389/fpls.2019.00307

Farquhar, G. D., Ehleringer, J. R., & Hubick, K. T. (1989). Carbon Isotope Discrimination and Photosynthesis. *Annual Review of Plant Physiology and Plant Molecular Biology*, *40*(1), 503–537. https://doi.org/10.1146/annurev.pp.40.060189.002443

Fonti, M. V., Vaganov, E. A., Wirth, C., Shashkin, A. V., Astrakhantseva, N. V., & Schulze, E.-D. (2018). Age-Effect on Intra-Annual δ13C-Variability within Scots Pine Tree-Rings from Central Siberia. *Forests*, *9*(6), 364. https://doi.org/10.3390/f9060364

25

Fonti, M. V., Von Arx, G., Harroue, M., Schneider, L., Nievergelt, D., Björklund, J., Hantemirov, R., Kukarskih, V., Rathgeber, C. B. K., Studer, N.-T., & Fonti, P. (2025). A protocol for high-quality sectioning for tree-ring anatomy. *Frontiers in Plant Science*, *16*, 1505389. https://doi.org/10.3389/fpls.2025.1505389

Gärtner, H., & Nievergelt, D. (2010). The core-microtome: A new tool for surface preparation on cores and time series analysis of varying cell parameters. *Dendrochronologia*, *28*(2), 85–92. https://doi.org/10.1016/j.dendro.2009.09.002

Gärtner, H., Schneider, L., & Cherubini, P. (2024). A New Workflow for Sampling and Digitizing Increment Cores. *Journal of Visualized Experiments*, *211*, 67098. https://doi.org/10.3791/67098

Gavrichkova, O., Proietti, S., Moscatello, S., Portarena, S., Battistelli, A., Matteucci, G., & Brugnoli, E. (2011). Short-term natural δ 13C and δ18O variations in pools and fluxes in a beech forest: The transfer of isotopic signal from recent photosynthates to soil respired CO_2. *Biogeosciences*, *8*(10), 2833–2846. https://doi.org/10.5194/bg-8-2833-2011

Gessler, A., Brandes, E., Buchmann, N., Helle, G., Rennenberg, H., & Barnard, R. L. (2009). Tracing carbon and oxygen isotope signals from newly assimilated sugars in the leaves to the tree-ring archive. *Plant, Cell & Environment*, *32*(7), 780–795. https://doi.org/10.1111/j.1365-3040.2009.01957.x

Gessler, A., Ferrio, J. P., Hommel, R., Treydte, K., Werner, R. A., & Monson, R. K. (2014). Stable isotopes in tree rings: Towards a mechanistic understanding of isotope fractionation and mixing processes from the leaves to the wood. *Tree Physiology*, *34*(8), 796–818. https://doi.org/10.1093/treephys/tpu040

Gharun, M., Hörtnagl, L., Paul-Limoges, E., Ghiasi, S., Feigenwinter, I., Burri, S., Marquardt, K., Etzold, S., Zweifel, R., Eugster, W., & Buchmann, N. (2020). Physiological response of Swiss ecosystems to 2018 drought across plant types and elevation. *Philosophical Transactions of the Royal Society B: Biological Sciences*, *375*(1810), 20190521. https://doi.org/10.1098/rstb.2019.0521

Gibbons, J. D., & Chakraborti, S. (2010). *Nonparametric Statistical Inference* (0 ed.). Chapman and Hall/CRC. https://doi.org/10.1201/9781439896129

Gričar, J., Jevšenak, J., Hafner, P., Prislan, P., Ferlan, M., Lavrič, M., Vodnik, D., & Eler, K. (2022). Climatic regulation of leaf and cambial phenology in Quercus pubescens: Their interlinkage and impact on xylem and phloem conduits. *Science of The Total Environment*, *802*, 149968. https://doi.org/10.1016/j.scitotenv.2021.149968

Grossiord, C., Buckley, T. N., Cernusak, L. A., Novick, K. A., Poulter, B., Siegwolf, R. T. W., Sperry, J. S., & McDowell, N. G. (2020). Plant responses to rising vapor pressure deficit. *New Phytologist*, *226*(6), 1550–1566. https://doi.org/10.1111/nph.16485

Grossiord, C., Granier, A., Ratcliffe, S., Bouriaud, O., Bruelheide, H., Checko, E., Forrester, D. I., Dawud, S. M., Finér, L., Pollastrini, M., Scherer-Lorenzen, M., Valladares, F., Bonal, D., & Gessler, A. (2014). Tree diversity does not always improve resistance of forest ecosystems to drought. *Proceedings of the National Academy of Sciences*, *111*(41), 14812–14815. https://doi.org/10.1073/pnas.1411970111

Helle, G., & Schleser, G. H. (2004). Beyond CO_2-fixation by Rubisco—An interpretation of 13C/12C variations in tree rings from novel intra-seasonal studies on broad-leaf trees. *Plant, Cell and Environment*, *27*(3), 367–380. https://doi.org/10.1111/j.0016-8025.2003.01159.x

Hentschel, R., Hommel, R., Poschenrieder, W., Grote, R., Holst, J., Biernath, C., Gessler, A., & Priesack, E. (2016). Stomatal conductance and intrinsic water use efficiency in the drought year 2003: A case study of European beech. *Trees*, *30*(1), 153–174. https://doi.org/10.1007/s00468-015-1284-2

Holmes, R. (1983). Computer-assisted quality control in tree-ring dating and measurement. *Tree-Ring Bulletin*, *43*, 69–78.

Hommel, R., Siegwolf, R., Zavadlav, S., Arend, M., Schaub, M., Galiano, L., Haeni, M., Kayler, Z. E., & Gessler, A. (2016). Impact of interspecific competition and drought on the allocation of new assimilates in trees. *Plant Biology*, *18*(5), 785–796. https://doi.org/10.1111/plb.12461

Jevšenak, J. (2019). Daily climate data reveal stronger climate-growth relationships for an extended European tree-ring network. *Quaternary Science Reviews*, *221*, 105868. https://doi.org/10.1016/j.quascirev.2019.105868

27

Jevšenak, J., & Levanič, T. (2018). dendroTools: R package for studying linear and nonlinear responses between tree-rings and daily environmental data. *Dendrochronologia*, *48*, 32–39. https://doi.org/10.1016/j.dendro.2018.01.005

Jucker, T., Grossiord, C., Bonal, D., Bouriaud, O., Gessler, A., & Coomes, D. A. (2017). Detecting the fingerprint of drought across Europe's forests: Do carbon isotope ratios and stem growth rates tell similar stories? *Forest Ecosystems*, *4*(1), 24. https://doi.org/10.1186/s40663-017-0111-1

Kagawa, A., Sugimoto, A., & Maximov, T. C. (2006). Intra-Annual Patterns of $\delta^{13}C$ and $\delta^{18}O$ in Tree Rings: Exploring the Seasonal Climate Signal. *Journal of Geophysical Research: Biogeosciences*, *111*(G3), G03012. https://doi.org/10.1029/2006JG000205

Knüsel, S., Peters, R. L., Haeni, M., Wilhelm, M., & Zweifel, R. (2021). Processing and Extraction of Seasonal Tree Physiological Parameters from Stem Radius Time Series. *Forests*, *12*(6), 765. https://doi.org/10.3390/f12060765

Kress, A., Young, G. H. F., Saurer, M., Loader, N. J., Siegwolf, R. T. W., & McCarroll, D. (2009). Stable isotope coherence in the earlywood and latewood of tree-line conifers. *Chemical Geology*, *268*(1–2), 52–57. https://doi.org/10.1016/j.chemgeo.2009.07.008

Li, W., Manzanedo, R. D., Jiang, Y., Ma, W., Du, E., Zhao, S., Rademacher, T., Dong, M., Xu, H., Kang, X., Wang, J., Wu, F., Cui, X., & Pederson, N. (2023). Reassessment of growth-climate relations indicates the potential for decline across Eurasian boreal larch forests. *Nature Communications*, *14*(1), 3358. https://doi.org/10.1038/s41467-023-39057-5

Magh, R.-K., Eiferle, C., Burzlaff, T., Dannenmann, M., Rennenberg, H., & Dubbert, M. (2020). Competition for water rather than facilitation in mixed beech-fir forests after drying-wetting cycle. *Journal of Hydrology*, *587*, 124944. https://doi.org/10.1016/j.jhydrol.2020.124944

Martínez-Sancho, E., Treydte, K., Lehmann, M. M., Rigling, A., & Fonti, P. (2022). Drought impacts on tree carbon sequestration and water use—Evidence from intra-annual tree-ring characteristics. *New Phytologist*, *236*(1), 58–70. https://doi.org/10.1111/nph.18224

28

Martínez-Vilalta, J., Cochard, H., Mencuccini, M., Sterck, F., Herrero, A., Korhonen, J., Llorens, P., Nikinmaa, E., Nole, A., Poyatos, R., & others. (2009). Hydraulic adjustment of Scots pine across Europe. *New Phytologist*, *184*(2), 353–364.

Maxwell, R. S., & Larsson, L.-A. (2021). Measuring tree-ring widths using the CooRecorder software application. *Dendrochronologia*, *67*, 125841. https://doi.org/10.1016/j.dendro.2021.125841

McCarroll, D., & Loader, N. J. (2004). Stable isotopes in tree rings. *Quaternary Science Reviews*, *23*(7–8), 771–801. https://doi.org/10.1016/j.quascirev.2003.06.017

Michelot-Antalik, A., Granda, E., Fresneau, C., & Damesin, C. (2019). Evidence of a seasonal trade-off between growth and starch storage in declining beeches: Assessment through stem radial increment, non-structural carbohydrates and intra-ring δ13C. *Tree Physiology*, *39*(5), 831–844. https://doi.org/10.1093/treephys/tpz008

Mitchell, P. J., O'Grady, A. P., Tissue, D. T., Worledge, D., & Pinkard, E. A. (2014). Co-ordination of growth, gas exchange and hydraulics define the carbon safety margin in tree species with contrasting drought strategies. *Tree Physiology*, *34*(5), 443–458. https://doi.org/10.1093/treephys/tpu014

Monserud, R. A., & Marshall, J. D. (2001). Time-series analysis of 13C from tree rings. I. Time trends and autocorrelation. *Tree Physiology*, *21*(15), 1087–1102. https://doi.org/10.1093/treephys/21.15.1087

Monson, R. K., Littlejohn, R. O., Hu, J., Schimel, D. S., & Trahan, N. A. (2018). Conifer Tree Rings as Recorders of Past Atmospheric Conditions. *Tree Physiology*, *38*(8), 1138–1151. https://doi.org/10.1093/treephys/tpy024

Monson, R. K., Szejner, P., Belmecheri, S., Morino, K. A., & Wright, W. E. (2018). Finding the seasons in tree ring stable isotope ratios. *American Journal of Botany*, *105*(5), 819–821. https://doi.org/10.1002/ajb2.1083

Nourtier, M., Chanzy, A., Cailleret, M., Yingge, X., Huc, R., & Davi, H. (2014). Transpiration of silver Fir (Abies alba mill.) during and after drought in relation to soil properties in a Mediterranean mountain area. *Annals of Forest Science*, *71*(6), 683–695. https://doi.org/10.1007/s13595-012-0229-9

29

Novick, K. A., Ficklin, D. L., Grossiord, C., Konings, A. G., Martínez-Vilalta, J., Sadok, W., Trugman, A. T., Williams, A. P., Wright, A. J., Abatzoglou, J. T., Dannenberg, M. P., Gentine, P., Guan, K., Johnston, M. R., Lowman, L. E. L., Moore, D. J. P., & McDowell, N. G. (2024). The impacts of rising vapour pressure deficit in natural and managed ecosystems. *Plant, Cell & Environment*, *47*(9), 3561–3589. https://doi.org/10.1111/pce.14846

Offermann, C., Ferrio, J. P., Holst, J., Grote, R., Siegwolf, R., Kayler, Z., & Gessler, A. (2011). The long way down–are carbon and oxygen isotope signals in the tree ring uncoupled from canopy physiological processes? *Tree Physiology*, *31*(10), 1088–1102. https://doi.org/10.1093/treephys/tpr093

O'Leary, M. H. (1995). Environmental effects on carbon fractionation in terrestrial plants. In E. Wada, T. Yoneyama, M. Minigawa, T. Ando, & B. D. Fry (Eds.), *Stable Isotopes in the Biosphere* (pp. 78–91). Kyoto University Press.

Pérez-de-Lis, G., Rathgeber, C. B. K., Fernández-de-Uña, L., & Ponton, S. (2022). Cutting tree rings into time slices: How intra-annual dynamics of wood formation help decipher the space-for-time conversion. *New Phytologist*, *233*(3), 1520–1534. https://doi.org/10.1111/nph.17869

Petek-Petrik, A., Petrík, P., Lamarque, L. J., Cochard, H., Burlett, R., & Delzon, S. (2023). Drought survival in conifer species is related to the time required to cross the stomatal safety margin. *Journal of Experimental Botany*, *74*(21), 6847–6859. https://doi.org/10.1093/jxb/erad352

Peters, R. L., Speich, M., Pappas, C., Kahmen, A., Von Arx, G., Graf Pannatier, E., Steppe, K., Treydte, K., Stritih, A., & Fonti, P. (2019). Contrasting stomatal sensitivity to temperature and soil drought in mature alpine conifers. *Plant, Cell & Environment*, *42*(5), 1674–1689. https://doi.org/10.1111/pce.13500

Peters, R. L., Steppe, K., Cuny, H. E., De Pauw, D. J. W., Frank, D. C., Schaub, M., Rathgeber, C. B. K., Cabon, A., & Fonti, P. (2021). Turgor – a limiting factor for radial growth in mature conifers along an elevational gradient. *New Phytologist*, *229*(1), 213–229. https://doi.org/10.1111/nph.16872

30

Pflug, E. E., Siegwolf, R., Buchmann, N., Dobbertin, M., Kuster, T. M., Günthardt-Goerg, M. S., & Arend, M. (2015). Growth cessation uncouples isotopic signals in leaves and tree rings of drought-exposed oak trees. *Tree Physiology*, *35*(10), 1095–1105. https://doi.org/10.1093/treephys/tpv079

Puhe, J. (2003). Growth and development of the root system of Norway spruce (Picea abies) in forest stands—A review. *Forest Ecology and Management*, *175*(1–3), 253–273. https://doi.org/10.1016/S0378-1127(02)00134-2

R Core Team. (2022). *R: A Language and Environment for Statistical Computing*. R Foundation for Statistical Computing. https://www.R-project.org/

Rathgeber, C. B. K. (2017). Conifer tree-ring density inter-annual variability – anatomical, physiological and environmental determinants. *New Phytologist*, *216*(3), 621–625. https://doi.org/10.1111/nph.14763

Rinne-Garmston, K. T., Tang, Y., Sahlstedt, E., Adamczyk, B., Saurer, M., Salmon, Y., Carrasco, M. D. R. D., Hölttä, T., Lehmann, M. M., Mo, L., & Young, G. H. F. (2023). Drivers of intra-seasonal $\delta^{13}C$ signal in tree-rings of *Pinus sylvestris* as indicated by compound-specific and laser ablation isotope analysis. *Plant, Cell & Environment*, *46*(9), 2649–2666. https://doi.org/10.1111/pce.14636

Rossi, S., Anfodillo, T., Čufar, K., Cuny, H. E., Deslauriers, A., Fonti, P., Frank, D., Gričar, J., Gruber, A., King, G., Krause, C., Morin, H., Oberhuber, W., Prislan, P., & Rathgeber, C. B. K. (2014). Wood formation in trees under climate change. *Nature Plants*, *3*.

Saurer, M., Sahlstedt, E., Rinne-Garmston, K. T., Lehmann, M. M., Oettli, M., Gessler, A., & Treydte, K. (2023). Progress in high-resolution isotope-ratio analysis of tree rings using laser ablation. *Tree Physiology*, *43*(5), 694–705. https://doi.org/10.1093/treephys/tpac141

Schollaen, K., Heinrich, I., & Helle, G. (2014). UV-laser-based microscopic dissection of tree rings—A novel sampling tool for delta C-13 and delta O-18 studies. *New Phytologist*, *201*, 1045–1055.

Schumann, K., Schuldt, B., Fischer, M., Ammer, C., & Leuschner, C. (2024). Xylem safety in relation to the stringency of plant water potential regulation of European beech, Norway spruce, and Douglas-fir trees during severe drought. *Trees*, *38*(3), 607–623. https://doi.org/10.1007/s00468-024-02499-5

31

Skomarkova, M. V., Vaganov, E. A., Mund, M., Knohl, A., Linke, P., Boerner, A., & Schulze, E. D. (2006). Inter-annual and seasonal variability of radial growth, wood density and carbon isotope ratios in tree rings of beech (Fagus sylvatica) growing in Germany and Italy. *Trees-Structure and Function*, *20*, 571–586.

Soudant, A., Loader, N. J., Bäck, J., Levula, J., Kljun, & N. (2016). Intra-annual variability of wood formation and δ13C in tree-rings at Hyytiälä, Finland. *Agricultural and Forest Meteorology*, *224*, 17–29. https://doi.org/10.1016/j.agrformet.2016.04.015

Tang, Y., Sahlstedt, E., Young, G., Schiestl-Aalto, P., Saurer, M., Kolari, P., Jyske, T., Bäck, J., & Rinne-Garmston, K. T. (2022). Estimating intraseasonal intrinsic water-use efficiency from high-resolution tree-ring $\Delta^{13}C$ data in boreal Scots pine forests. *New Phytologist, 237*(5), 1606–1619. https://doi.org/10.1111/nph.18649

Torbenson, M. C. A., Stagge, J. H., Chen, F., Ziaco, E., & Esper, J. (2024). Adjusting the significance of daily climate responses in tree-ring proxies. *Journal of Forestry Research*, *36*(1). https://doi.org/10.1007/s11676-024-01799-3

Treydte, K., Liu, L., Padrón, R. S., Martínez-Sancho, E., Babst, F., Frank, D. C., Gessler, A., Kahmen, A., Poulter, B., Seneviratne, S. I., Stegehuis, A. I., Wilson, R., Andreu-Hayles, L., Bale, R., Bednarz, Z., Boettger, T., Berninger, F., Büntgen, U., Daux, V., … Loader, N. J. (2024). Recent human-induced atmospheric drying across Europe unprecedented in the last 400 years. *Nature Geoscience*, *17*(1), 58–65. https://doi.org/10.1038/s41561-023-01335-8

Unterholzner, L., Castagneri, D., Cerrato, R., Știrbu, M.-I., Roibu, C.-C., & Carrer, M. (2024). Climate response of a glacial relict conifer across its distribution range is invariant in space but not in time. *Science of The Total Environment*, *906*, 167512. https://doi.org/10.1016/j.scitotenv.2023.167512

Vaganov, E. A., Schulze, E.-D., Skomarkova, M. V., Knohl, A., Brand, W. A., & Roscher, C. (2009). Intra-annual variability of anatomical structure and delta(13)C values within tree rings of spruce and pine in alpine, temperate and boreal Europe. *Oecologia*, *161*(4), 729–745. https://doi.org/10.1007/s00442-009-1421-y

32

Vitali, V., Büntgen, U., & Bauhus, J. (2017). Silver fir and Douglas fir are more tolerant to extreme droughts than Norway spruce in south-western Germany. *Global Change Biology*, *23*(12), 5108–5119. https://doi.org/10.1111/gcb.13774

Vitali, V., Klesse, S., Weigt, R., Treydte, K., Frank, D., Saurer, M., & Siegwolf, R. T. W. (2021). High-frequency stable isotope signals in uneven-aged forests as proxy for physiological responses to climate in Central Europe. *Tree Physiology*, *41*(11), 2046–2062. https://doi.org/10.1093/treephys/tpab062

Walthert, L., Etzold, S., Carminati, A., Saurer, M., Köchli, R., & Zweifel, R. (2024). Coordination between degree of isohydricity and depth of root water uptake in temperate tree species. *Science of The Total Environment*, *946*, 174346. https://doi.org/10.1016/j.scitotenv.2024.174346

Walthert, L., & Meier, E. S. (2017). Tree species distribution in temperate forests is more influenced by soil than by climate. *Ecology and Evolution*, *7*(22), 9473–9484. https://doi.org/10.1002/ece3.3436

Walthert, L., & Schleppi, P. (2018). Equations to compensate for the temperature effect on readings from dielectric *Decagon MPS-2* and *MPS-6* water potential sensors in soils. *Journal of Plant Nutrition and Soil Science*, *181*(5), 749–759. https://doi.org/10.1002/jpln.201700620

Wieloch, T., Holloway-Phillips, M., Yu, J., & Niittylä, T. (2024). New insights into the mechanisms of plant isotope fractionation from combined analysis of intramolecular [13] C and deuterium abundances in *Pinus nigra* tree-ring glucose. *New Phytologist*, nph.20113. https://doi.org/10.1111/nph.20113

Wigley, T., Briffa, K. R., & Jones, P. D. (1984). On the Average Value of Correlated Time Series, with Applications in Dendroclimatology and Hydrometeorology. *American Meteorological Society*, *23*(2), 201–213.

Winkler, A., & Oberhuber, W. (2017). Cambial response of Norway spruce to modified carbon availability by phloem girdling. *Tree Physiology*, *37*(11), 1527–1535. https://doi.org/10.1093/treephys/tpx077

Xu, G., Liu, X., Hu, J., Dorado-Liñán, I., Gagen, M., Szejner, P., Chen, T., & Trouet, V. (2022). Intra-annual tree-ring δ18O and δ13C reveal a trade-off between isotopic source and humidity in moist environments. *Tree Physiology*, tpac076. https://doi.org/10.1093/treephys/tpac076

33

Zelenov, G. K., Belokopytova, L. V., Babushkina, E. A., Zhirnova, D. F., Yang, B., Peng, X., Liu, J., Sitnikov, G. A., & Vaganov, E. A. (2024). Reconstruction of Seasonal Kinetics in Conifer Radial Growth from Daily Meteorological Conditions, Tree-Ring Width, and Radial Size of Tracheids. *Forests*, *15*(2), 249. https://doi.org/10.3390/f15020249

Zhang, Y., Chen, H. Y. H., & Reich, P. B. (2012). Forest productivity increases with evenness, species richness and trait variation: A global meta-analysis. *Journal of Ecology*, *100*(3), 742–749. https://doi.org/10.1111/j.1365-2745.2011.01944.x

Ziaco, E. (2020). A phenology-based approach to the analysis of conifers intra-annual xylem anatomy in water-limited environments. *Dendrochronologia*, *59*.

Zweifel, R., Etzold, S., Basler, D., Bischoff, R., Braun, S., Buchmann, N., Conedera, M., Fonti, P., Gessler, A., Haeni, M., Hoch, G., Kahmen, A., Köchli, R., Maeder, M., Nievergelt, D., Peter, M., Peters, R. L., Schaub, M., Trotsiuk, V., … Eugster, W. (2021). TreeNet–The Biological Drought and Growth Indicator Network. *Frontiers in Forests and Global Change*, *4*, 776905. https://doi.org/10.3389/ffgc.2021.776905

Zweifel, R., Haeni, M., Buchmann, N., & Eugster, W. (2016). Are trees able to grow in periods of stem shrinkage? *New Phytologist*, *211*(3), 839–849. https://doi.org/10.1111/nph.13995

Zweifel, R., Item, H., & Hasler, R. (2001). Link between diurnal stem radius changes and tree water relations. *Tree Physiology*, *21*(12–13), 869–877. https://doi.org/10.1093/treephys/21.12-13.869

Zweifel, R., Sterck, F., Braun, S., Buchmann, N., Eugster, W., Gessler, A., Häni, M., Peters, R. L., Walthert, L., Wilhelm, M., Ziemińska, K., & Etzold, S. (2021). Why trees grow at night. *New Phytologist*, *231*(6), 2174–2185. https://doi.org/10.1111/nph.17552
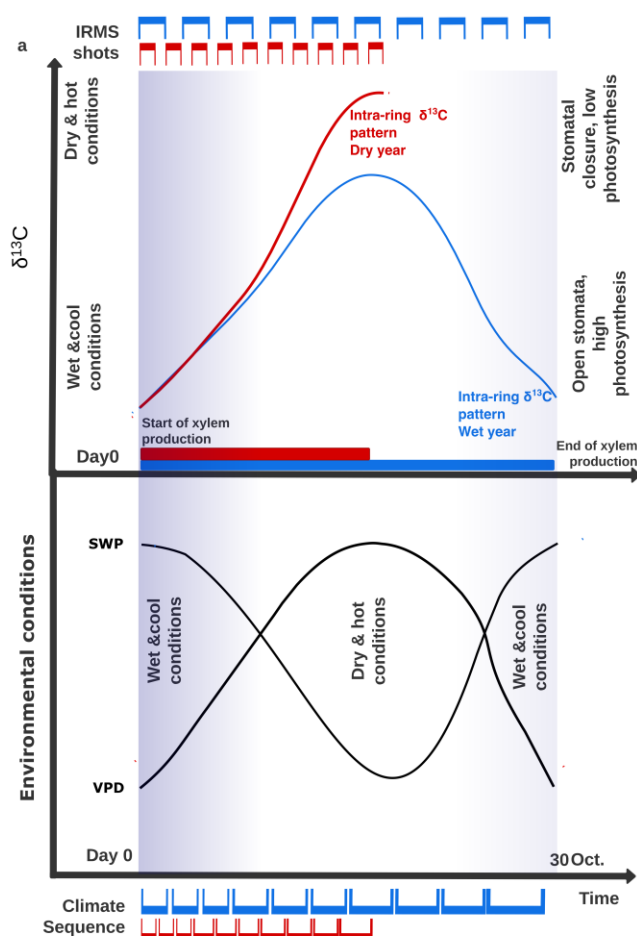
34

List of figures

Fig. 1 Conceptual diagram illustrating (a) δ¹³C intra-ring patterns observed from high-resolution LA-IRMS, with the 10-shots sequence creating a sequential sampling of the whole ring. The δ13C variation reflects seasonal changes in stomatal regulation and photosynthetic rates in response to seasonal environmental conditions (b) of atmospheric and soil dryness. In wet and cold years, high stomatal conductance and photosynthesis produce a characteristic "bell-shaped" δ¹³C curve (blue δ¹³C line). In contrast, hot and dry conditions induce tighter stomatal control and reduced photosynthesis, resulting in a steep δ¹³C increase from earlywood to latewood, forming a distinctive "monotonic rise" pattern (red δ13C line). (b) Schematic representation of the sequential division of seasonal environmental data into 10 windows, anchored to Day 0 (the onset of stem formation). The highest cross-correlation between δ¹³C and environmental variables, such as vapour pressure deficit (VPD) and soil water potential (SWP), allows for the identification of the xylem-integrated seasonal environmental information. Red windows represent the selection for hot and dry years (corresponding to monotonic rise pattern of δ¹³C), which indicates an earlier end of xylem formation. Blue windows represent wet and cool years (corresponding to "bell-shaped" δ¹³C curves), which indicate longer xylem, reflecting later-season environmental information.
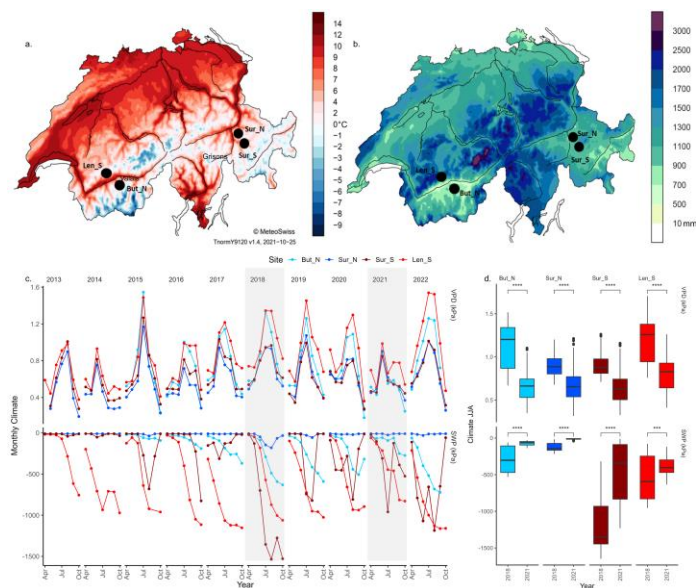
35

*Fig.1 Locations of the sampled sites on maps of (a) mean yearly temperature and (b) mean yearly precipitation (1991-2020, MeteoSwiss). (c) Monthly vapour pressure deficit (VPD, kPa) and soil water potential at 80 cm depth (SWP, kPa), smoothed with a two-week running average for the growing season (April to October) for each year, comparison with temperature and precipitation are shown in Fig S.2. The years 2018 and 2021 are highlighted and used for further comparisons, which combined the lowest SWP and highest VPD conditions for all sites.(d) comparison of summer VPD and SWP of the two selected years (2018, 2014). Significant differences between pairs are indicated by asterisks (P<0.0001=****).*
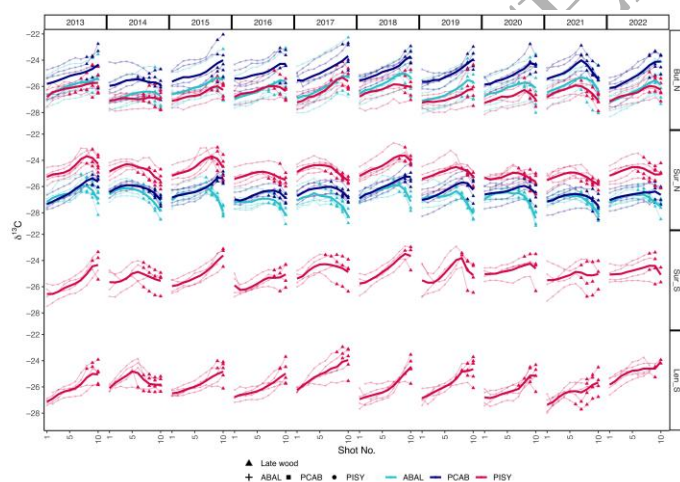
Fig.2 Intra-annual tree-level (thin lines) and average (bold lines) $\delta^{13}C$ measurements for the years 2013–2022 for the sampled species (Abies alba (ABAL), Picea abies (PCAB), and Pinus sylvestris (PISY)), at the respective sites (for details, see Table 1). The latewood points have a dedicated shape. The earlywood and latewood boundaries for each tree are shown in Fig. S.4. Descriptive statistics for inter-series correlations and the expressed population signal (EPS) are given in Table S.3.
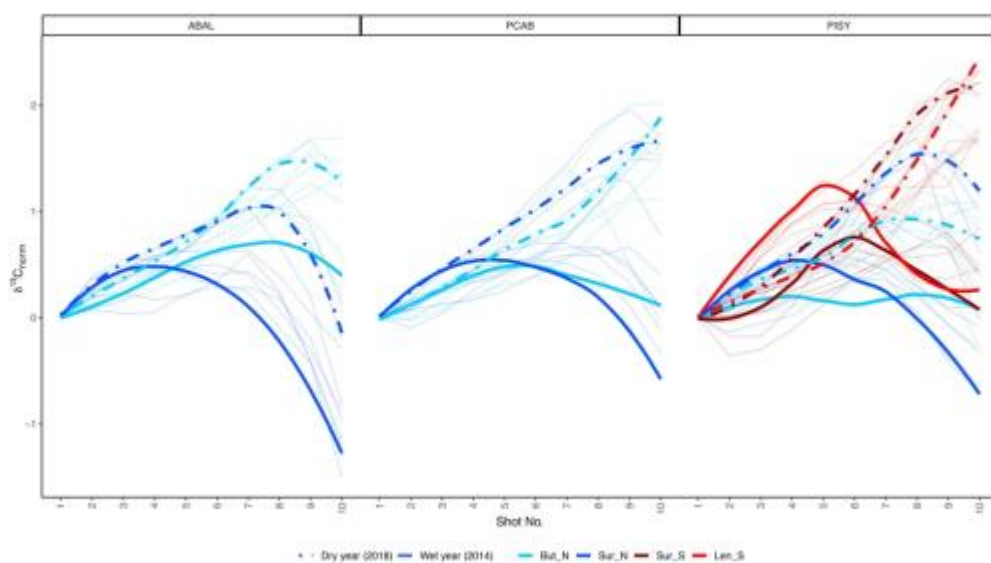
Fig.3 δ¹³C species-specific loess smoothed curves for Abies alba (ABAL), Picea abies (PCAB), and Pinus sylvestris (PISY) for the wet (2021) and dry (2018) years. A prominent and consistent bell-shaped and monotonic rise pattern appeared across the four sites. Comparisons across all years are shown in Fig. S.5, and comparisons with monthly means are shown in Fig. S.6.
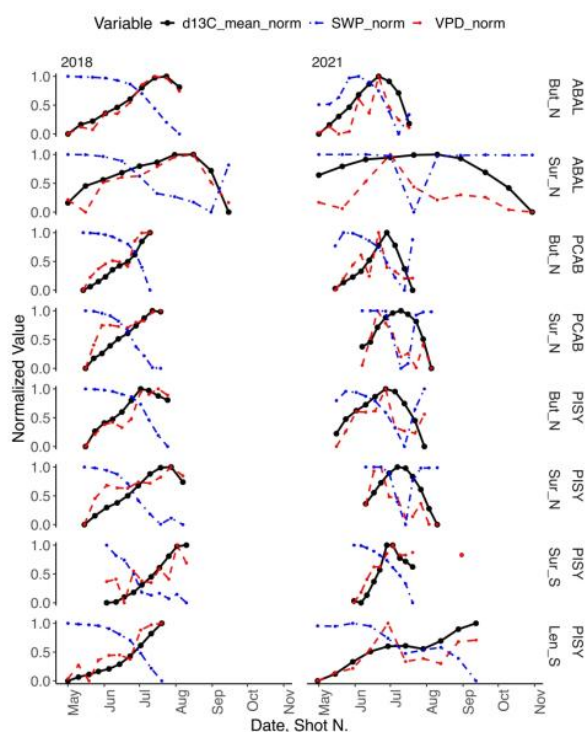

Fig.4 Resulting curves for the normalized environmental variables and δ¹³C time series, restricted to dates between Day0 and the optimum End date and averaged into 10 time windows aligned to the 10 δ¹³C shots. If multiple maxima occurred, the

37

average date was used. The complete results for cross-correlations, end-date result selection, and non-normalized optimized time series for all years are shown in Fig.S.6,S.7.
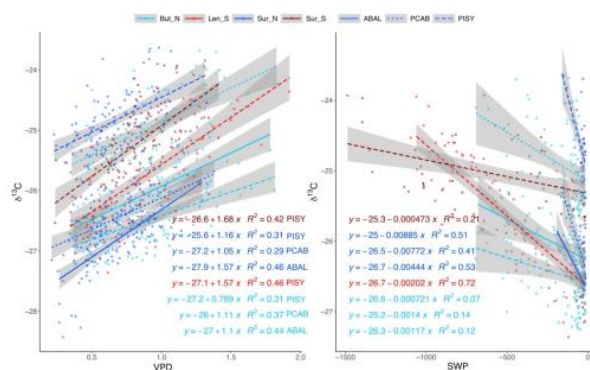

Fig.5 Site and species mean $\delta^{13}C$ shot values and their relationship with the sequence-dependent averages of vapour water deficit (VPD) and soil water potential (SWP) at 80 cm depth, according to the selected window sequence and aligned to Day0 and End date (the non-aligned correlation can be found in Fig. S.8). Linear models were fitted for each species and site. Model equations and explained variance (R^2) are indicated. For SWP, values between -0 and -15 were removed for the model to focus on dry conditions at all sites (all data shown in Fig. S.9).
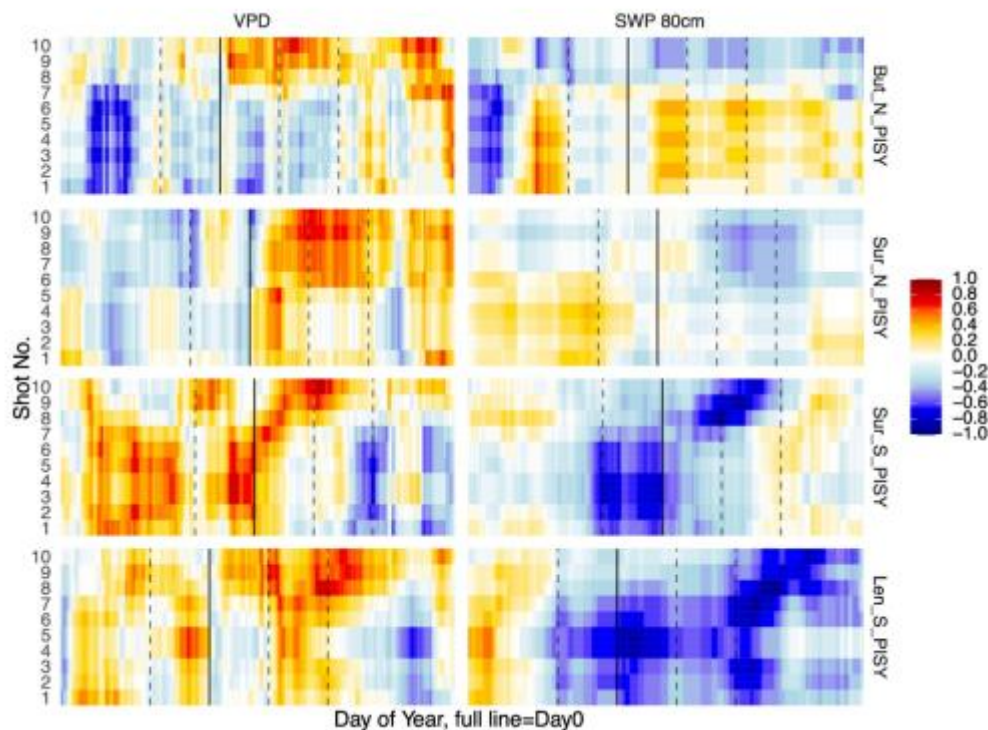

Fig.6 Heatmaps displaying Kendall's tau correlation coefficients between $\delta^{13}C$ values measured in the 10 consecutive shots in tree-rings (y-axes) and vapour pressure deficit (VPD, left panels) and soil water potential at 80 cm depth (SWP 80 cm, right

38

panels), aggregated into 20-day moving windows for Pinus sylvestris across all sites. The x-axis represents the day of the year, with solid vertical lines indicating Day 0 and dashed lines indicating 50 days before and 50 and 100 days after Day0. The staggering of the solid line across the panels reflects the difference in the start date for growth among the species at each site. All species responses are in Fig.S11.

39